v. 3, n. 35, 2023

Journal of
Engineering
Research

ANALYSIS OF SUBSYNCHRONOUS RESONANCE VIA TORSIONAL INTERACTIONS IN ELECTROMECHANICAL SYSTEMS THROUGH DIFFERENT FAULT POINTS

Carlos HSM Junior
DEELE
CEFET-RJ
Rio de Janeiro-RJ, Brazil

João A. Moor Neto
DEELE
CEFET-RJ
Rio de Janeiro-Rj, Brazil

Gustavo K. Dill
DE MET
CEFET-RJ
Rio de Janeiro-Rj, Brazil

All content in this magazine is licensed under a Creative Commons Attribution License. Attribution-Non-Commercial-Non-Derivatives 4.0 International (CC BY-NC-ND 4.0).

Abstract: This article investigates the occurrence of Subsynchronous Resonance (RSS) in power systems composed of a turbine-generator set and electrical network with the presence of series compensation in an alternative way, through different fault points. The set is represented in the form of state space to allow modal analysis and obtain the natural oscillation frequencies of the system. The study proposal aims to analyze the influence of the location of the fault and the impact of this premise on the accentuation of existing torsional interactions during the occurrence of RSS. The simulations were carried out in the PSCAD/EMTDC environment, applying three-phase faults at different points of the equivalent system. There is an occurrence of energy exchange related to the occurrence of Subsynchronous Resonance via Torsional Interactions, for the fault scenarios analyzed.
Keywords: Subsynchronous Resonance ; Torsional Interactions; Series Compensation; Mohave.

INTRODUCTION

Series compensation is a widespread methodology to increase electrical energy transfer capacity, optimize the voltage profile and improve system stability [1]. However, its use may result in an electrical or electromechanical condition of the system in which the electrical network exchanges significant energy with the turbine-generator set at one or more natural frequencies of the combined system, below the synchronous frequency, and subsequent to a disturbance having as initial condition equilibrium, a phenomenon known as Subsynchronous Resonance (RSS) [2], [3]. This oscillation condition, due to its complexity, is divided into three manifestations: the Induction Generating Effect (IGE), Torsional Interactions (TI) and Torque Amplification (TA) [4]. The first two are forms of self-excitation, the first being purely electrical and the second electromechanical [5]. Furthermore, the third manifestation has an intrinsic relationship with disturbances in the network related to transient torques. The three manifestations have their own origins, but they can coexist or even culminate in the existence of another [6], especially in power systems with the existence of thermoelectric turbogenerators, the focus of the study presented.

The thermoelectric turbogenerator is considered to have a complex mechanical structure, connecting several rotating masses through a non-rigid shaft [7]. When the system is affected per intense disturbances, one notices the emergence of torsional oscillations between the different rotating masses. This type of disturbance, when related to series compensated systems [8], results in the approximation between the natural frequency bands of the turbogenerator and the natural frequencies of the network, at a level lower than the synchronous frequency. In the case of the aforementioned condition, the coincidence between the frequencies of the turbogenerator-grid set influences electromechanical interactions and involuntary energy exchange. The scenario addressed characterizes the existence of subsynchronous oscillation phenomena, such as, for example, Subsynchronous Resonance.

On 12/9/1970 and 10/26/1971, the most damaging impacts of electromechanical oscillations ever witnessed to date were witnessed. The two generators of the Mohave thermoelectric generating unit (California, USA) were completely fatigued by Subsynchronous Resonance via Torsional Interactions [9]. After the series of incidents that occurred, the electrical industry passed a milestone in terms of compensation. Before the incident, series compensation in long transmission lines was used without detailed sizing, without taking into account

the mechanical interactions between the turbine-generator set and the electrical grid, which culminated in several studies of the phenomenon of Subsynchronous Resonance, in global level.

When it comes to studies related to Subsynchronous Resonance via Torsional Interactions, the literature prioritizes the analysis of the degree of compensation adopted for the system [10] and [11], with extremely important factors such as the location of the fault occurring without the necessary approach. On the other hand, this study's main contribution is to approach the oscillatory phenomenon from the perspective of fault location. Thus, two different points were considered for the application of faults in the same system in order to compare and investigate the impacts that exist during Torsional Interactions. To this end, the Mohave electromechanical power system, developed for simulations by [10] and [11] during incidents in the PSCAD / EMTDC environment [12], is reproduced, with the insertion of the three-phase fault parameterized for the occurrence of Torsional Interactions at one of the natural frequencies of the turbogenerator. In this particular study, faults are applied at two different points in the system, specifically before and after series compensation. Therefore, focus was given to a comparative analysis of results obtained in simulations to investigate the RSS phenomenon. It must be noted that the analysis was directed to the torques of the turbogenerator shaft and magnitudes of the specified series capacitor.

In addition to the introduction presented in this chapter, in chapter II dynamic modeling is introduced to obtain the frequencies of the torsional modes of the set, in chapter III the focus is given to modeling the system in a PSCAD/EMTDC environment [12], in chapter IV the results considering the application of the fault at two different points and in chapter V the conclusions of the analysis are presented.

DYNAMICS OF THE ELECTROMECHANICAL SYSTEM

In the dynamics of the turbine-generator + electrical grid system, the mechanical part of the system provides the position and speed of the rotor (turbogenerator axis) as a function of the mechanical torque, exciting the electrical system, depending on the degree of series compensation, which reacts to the mechanical excitations through the electrical torque.

For the study of Subsynchronous Resonance, it is important to treat the turbogenerator as a multi-mass -spring system, considering the shaft stiffness constants (equivalent to the elastic stiffness constants of the traditional mass-spring model) and the mutual damping of the mass zones. [13]. The system can have more than one natural frequency, given the different sections and mechanical parameters that make up the shaft. Each section can have an oscillation mode. The multi- spring model presented in this work is based on [14]. An imaginary section of the turbogenerator shaft is considered, with a set of mass zones given by *n= [1,....,m],* with inertia constants H_n, damping coefficients of their own D_n and, with mutual elastic constants $K_{n,n+1}$ as represented in Figure 1.

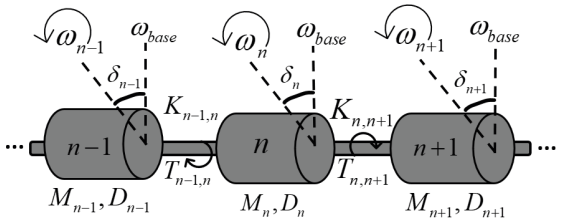

Figure 1. Multi-mass-spring model of the turbogenerator shaft.

Expressions (1) and (2) represent the interactions between the mass zones.

$$2H_n \frac{d(\Delta\omega_n)}{dt} = T_n - D_n(\Delta\omega_n) - T_e - K_{n,n+1}(\delta_{n+1} - \delta_n) + k_{n-1,n}(\delta_n - \delta_{n-1}) \quad (1)$$

$$\frac{d(\delta_n)}{dt} = \omega_b.(\Delta\omega_n) \quad (2)$$

For the mass zone of the generator, the mass zone torque T_n and the mutual elastic constant after the generator $K_{n-1,n}$ $(\delta_n - \delta_{n-1})$ do not exist and for the other low, medium and high pressure stages the electrical torque T_e ceases to exist. The angle δ_n represents the angular difference between the mass zone velocity and the reference angular velocity ω_b.

The linearized rotor equations can be readily written from equations (1) and (2) in order to obtain their representation in state space form. For small disturbances in the system, the electrical torque of the generator can be expressed as a function of the synchronizing torque coefficient K_m so that $T_e = K_m \cdot \Delta\delta_m$. Equivalently to equation (1), the linearized equation that describes the interactions between the mass zones is represented by expressions (3) and (4):

$$2H_n \frac{d(\Delta\omega_n)}{dt} = -D_n(\Delta w_n) - k_{n,n+1}(\delta_{n+1}) - -k_{n-1,n}(\delta_{n-1}) + (K_{n-1,n} + k_{n,n+1})(\delta_n) \quad (3)$$

$$\frac{d(\Delta\delta_n)}{dt} = \omega_b.(\Delta\omega_n) \quad (4)$$

In an equivalent way to what is stated in equation (1), for the mass zone of the generator the component $(K_{n-1,n} + K_{n,n+1}$ (δ_n) does not already exist, for the mass zones that do not involve the generator the synchronizing torque coefficient K_m is null. Equation (3) can be rewritten in a simplified form to perform the modal analysis as given in (5):

$$M\frac{d(\Delta w_n)}{dt} = -D(\Delta w_n) - K(\delta_n) \quad (5)$$

Where, $M = 2\frac{H}{\omega_b}$ $[Kg \times m^2]$ is a diagonal matrix of rotational mass of the inertia constant, D is a diagonal matrix with the damping coefficients, K is a trigonal matrix composed of the proper and mutual constants between the mass zones of the system and ω_b is the base synchronous speed of the system used as a reference parameter. The damping coefficients are sized by field tests for specific operating conditions, which makes the sizing of these parameters non-trivial.

In order to obtain the *mode -shapes* of the system, the natural frequencies, as well as their oscillations, the state matrix of the system is determined through the matrix calculation of equation (5), disregarding the damping coefficients of the machines as per expression (6).

$$A = M^{-1}K \quad (6)$$

Where, the M and K matrices are determined by equations (7) and (8) and, each state represents a mass zone:

$$M = \begin{bmatrix} \frac{2H_{nn}}{w_b} & 0 & 0 & 0 \\ 0 & \frac{2H_{nn}}{w_b} & 0 & 0 \\ 0 & 0 & \ddots & 0 \\ 0 & 0 & 0 & \frac{2H_{mm}}{w_b} \end{bmatrix} \quad (7)$$

$$K = \begin{bmatrix} k_{n,n+1} & -k_{n,n+1} & 0 & 0 \\ -k_{n,n-1} & k_{n-1,n} + k_{n,n+1} & -k_{n,n+1} & 0 \\ 0 & -k_{n,n-1} & \ddots & \dots \\ 0 & 0 & \vdots & k_{m-1,m} \end{bmatrix} \quad (8)$$

The intersection between two frequency bands is proportional to the degree of series compensation, a crucial factor for the occurrence of Subsynchronous Resonance via Torsional Interactions [14]. The difference between the synchronous frequency and the natural frequency of the electrical grid tends to excite the torsional modes of the turbine-generator set [15]. This difference causes the conjugate to operate subsynchronously. If this is greater than the mechanical damping torque of the turbogenerator shaft at the resonance frequency, the electromechanical system is subject to increasing oscillations, characterizing a condition of instability,

so that the subsynchronous torque causes negative damping. To define the scenario for the occurrence of this manifestation of Subsynchronous Resonance, it is necessary to compare four frequencies of the electromechanical system: the synchronous frequency, the frequency value of the series capacitor, the natural frequency value of the network (f_n^{REDE}) and the frequency value of the torques of the turbogenerator shaft (f_n^{TURB}), as represented in the flowchart in Figure 2.

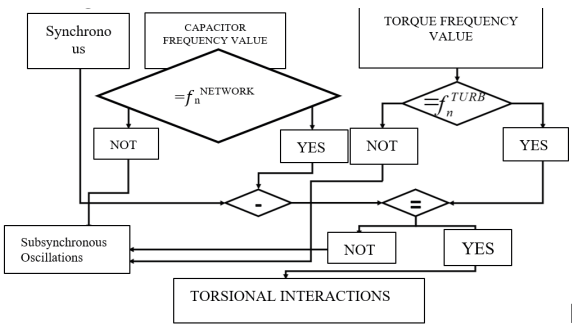

Figure 2. Flowchart of the conditions for the occurrence of Torsional Interactions.

Given that the network frequency, the synchronous frequency and the frequency set for the capacitor are known, the torsional interactions are verified by comparing with the frequencies of the modes of the turbine-generator set, obtained from the electromechanical modes of matrix A, described in equation (6).

SYSTEM PARAMETERIZATION

In incidents that occurred at the Mohave thermoelectric plant between 1970 and 1971, the turbine-generator set of the generating unit was affected by Subsynchronous Resonance via Torsional Interactions. As at the time the sizing of series compensation had no restrictions, the degree of compensation of the electromechanical system was 74%, according to the sizing proposed in [16]. In this chapter the case of Subsynchronous Resonance will be reproduced, introducing a comparative analysis between the two possible locations of the fault occurrence: before and after series compensation. The simulations were carried out using the PSCAD/EMTDC software [12] and the obtaining of mechanical parameters necessary to enable the investigation of Torsional Interactions was developed in the MATLAB software [17].

CASE STUDY

The turbine-generator set used in Mohave (1970-71) has 892.4 MVA, with 4 pressure zones (one high, one medium and two low), generator and exciter. Therefore, the model presented in chapter II is expanded to five states. Figure 3 illustrates the system adopted by [10] for representation and analysis of the set, with the possibility of applying faults at points A and B.

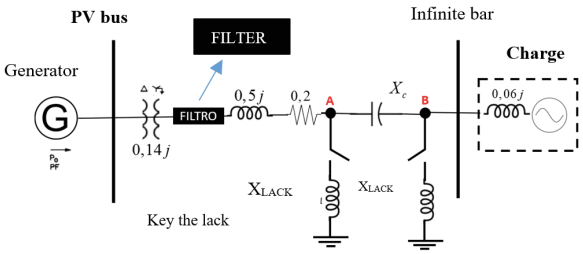

Figure 3. Schematic of the Mohave power system in the years 1970 and 1971.

The electrical and mechanical parameters of the turbine-generator set are presented in Tables I and II. In Table I the reactance data in the direct and quadrature axes for the periods of steady state *X*, transient regime *X′* and subtransient regime *X″* , as well as their respective equivalent time constants *T, T′ e T″*. In Table II, there are the inertia constants *H,* for the different zones of mass, in addition to the damping coefficients *D* and also the mutual torsional constants *K*.

GENERATOR – 892.4 MVA (VALUES IN PU)		
$X_d = 1,79$	$X'_d = 0,169$	$X''_d = 0,135$
$X_q = 1,71$	$X'_q = 0,228$	$X''_q = 0,2$
$X_L = 0,13$	$R_1 = 0$	$T'_{d0} = 4,3$
$T''_{d0} = 0,032$	$T'_{q0} =$	$T''_{q0} = 0,05$

TABLE I. Impedances and Time Constants [10]

PASTA	H	D	ADJACENCIES	K
HP	0.092897	0.104108	**HP-IP**	19,303
IP	0.155589	0.058477	**IP-LPA**	34,929
LPA	0.858670	0.019680	**LPA-LPB**	52,038
LPB	0.884215	0.002280	**LPB-GER**	70,858
GER	0.868495	0.024762	**GER-EXC**	2,822
EXC	0.0342165	0.010219		

Table II. DYNAMIC DATA OF THE TURBOGENERATOR SHAFT (in PU) [10]

In steady state, the distribution of mechanical torque across the shaft sections is given by the respective proportion: 30% High Pressure (HP), 26% Medium Pressure (IP), 22% Low Pressure of stage A (LPA), 22% Low Pressure stage B (LPB). The Generator constants (GEN) and the exciter constants (EXC) are also presented in Table II. The exciter torque is assumed null so that initial fatigue between the adjacency is not considered [10].

COMPUTATIONAL IMPLEMENTATION

To obtain the natural frequencies and analyze the Subsynchronous Resonance, the MATLAB program [17] was used to carry out the Modal Analysis. From the adopted turbogenerator parameters, the matrices [A], [K] and [M] are determined, and from the Eigenvalues of [A], the natural oscillation frequencies of the turbogenerator are obtained. If the system's complementary frequency coincides with one of the five mechanical natural frequencies, the system will enter the RSS instability zone.

To adapt the case study in the PSCAD/EMTDC environment [12], it is considered that the generator operates with an initial power of 0.9 pu and an inductive power factor of 90%. Three-phase faults (phase-to-ground) with a reactance of 0.04 are applied pu and duration of 0.075 seconds. The series capacitor has a reactance of 0.371 pu and the inductive reactance of the line is 0.5 pu [10]. The values in pu are established depending on the magnitudes of the adopted turbogenerator. The fault is entered into the system in 1.5 seconds. The turbine-generator set described in the previous section connects to a series compensated 539kV line. This connection is made by a star-delta transformer (539kV/26kV). The synchronous machine has a phase voltage of 15.011kV and the simulation time is nine seconds. At the moment the fault occurs (1.5 seconds), the multi-mass block representing the mechanical part of the turbogenerator is associated with the synchronous machine, with constant synchronous speed. The machine field voltage is assumed constant. The mutual damping and damping specific to the multimass block were disregarded, aiming to observe the oscillatory phenomenon *in natura*. The analysis of the frequency value of the stationary quantities of the series capacitor is carried out via the Fast Fourier Transform FFT (*Fast Fourier Transform*) [18]. Figures 4 and 5 illustrate, respectively, the turbogenerator and the electrical network, with the respective appropriate parameterizations in the PSCAD/EMTDC environment [12].

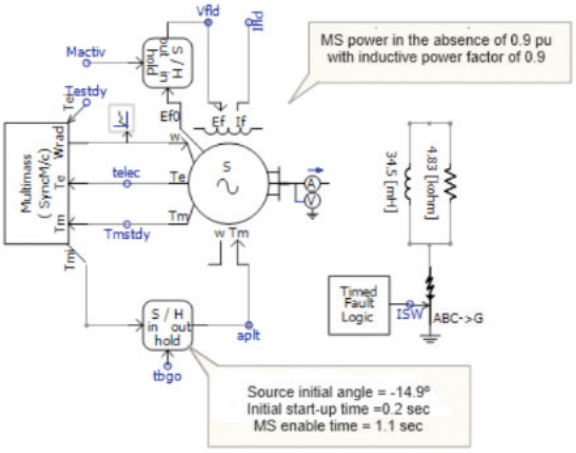

Figure 4. Representation of the turbogenerator and the fault in a PSCAD/EMTDC environment [12].

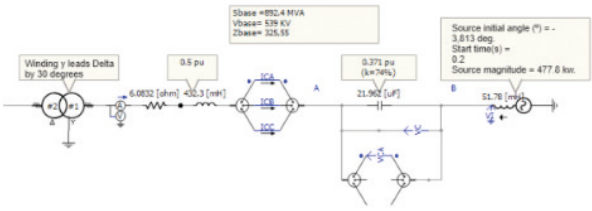

Figure 5. Representation of the electrical network with series compensation in the PSCAD/EMTDC environment [12], with two points (A and B) for fault applications.

RESULTS

The results are presented through comparative analysis of the effect of the fault, applied at different points, on the electrical quantities of the system. The oscillatory frequency of the synchronous machine's torque quantities, capacitor voltage, torque in the mass zones, among others, are observed.

In this study, the system parameters indicated in chapter III are inserted into the modeling presented in chapter II in order to obtain the oscillation modes of the turbine-generator set and their respective natural frequencies of $()f_n$. Such frequencies, obtained through the imaginary part of the eigenvalues of matrix A, are presented in Table III:

f_n 1	f_n 2	f_n 3	f_n 4	f_n 5
15,718	20.2121	25.5508	32.2929	47.4563

TABELA III. NATURAL TURBOTGERATOR OSCILLATION FREQUENCIES IN HERTZ

In order to obtain the RSS, via torsional interactions, the capacitor voltage frequency is adjusted to 40Hz. Thus, the system's complementary frequency (60Hz – 40Hz) is sufficiently close to the natural oscillation frequency of the turbine-generator set presented in the second oscillation mode of Table III. For this condition, a fault is applied before and after the capacitor and the behavior of the electrical quantities in the set is evaluated.

FOUL APPLIED AT POINT B

For the fault application scenario after the series capacitor, a sharp increase in the machine torque was observed, as shown in Figure 6.

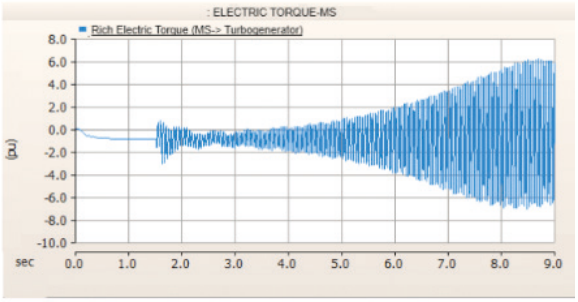

Figure 6. Electrical torque in the Synchronous Machine.

During the fault, there is a sharp increase in the voltages and currents of the series capacitor. However, even after the fault duration ended, overvoltages and overcurrents were observed. The voltage magnitude reaches values close to 2000 pu as illustrated in Figure 7. It was also found that the speed of the turbine-generator set also increased too much due to disturbances during and after the fault.

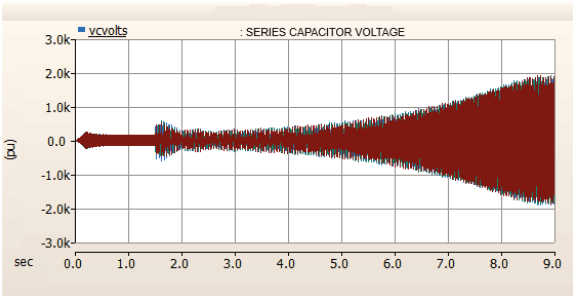

Figure 7. Voltage across the series capacitor.

The electrical torques between the adjacencies of the turbogenerator shaft suffer disturbances in their magnitudes during the application of the fault, in 1.5 seconds. However, after extinguishing this, a completely inappropriate behavior of the turbogenerator is noticed, the main result of the system's self-excitation. The adjacencies are treated in detail in Figures 8, 9, 10, 11 and 12, respectively. The existence of torque between the exciter and the generator is observed, in line with the distribution of torques in the turbogenerator during equilibrium, as shown in Figure 8. The torque between generator and exciter will be treated prominently, given the mass arrangement of these sections. There is an increase in torque between the entire turbogenerator shaft. The two largest torsional interactions occur between the two low pressure zones (37.96 pu peak torque) and the generator and exciter (32.86 pu peak). The entire axis remained stressed, even after the fault, a typical scenario for the occurrence of Subsynchronous Resonance.

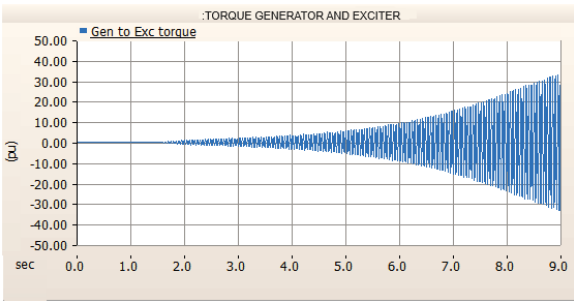

Figure 8. Torque between the Generator and Exciter.

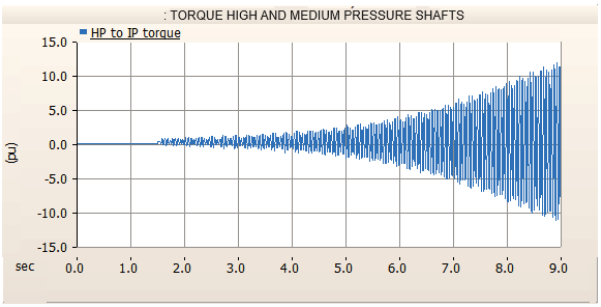

Figure 9. Torque between the High and Medium Pressure Zones.

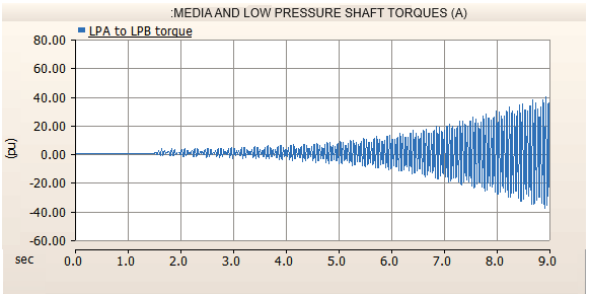

Figure 10. Torque between the Medium and Low Pressure Zones A.

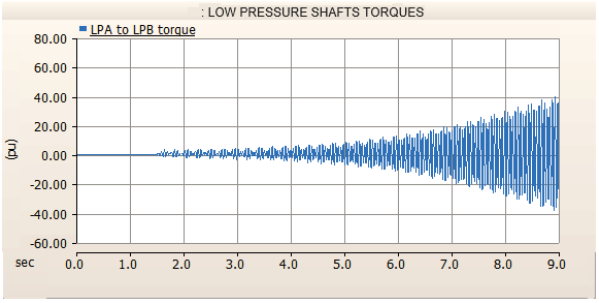

Figure 11. Torque between Low Pressure Zones.

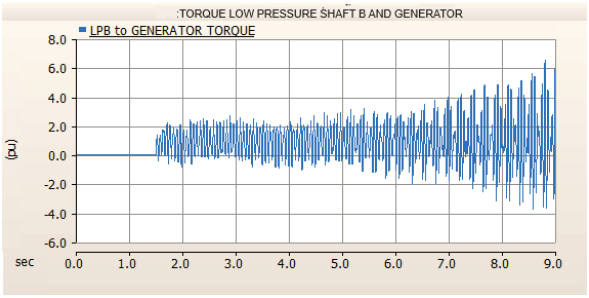

Figure 12. Torque between Low Pressure Zone B and Generator.

To investigate the frequency of the predominant voltage in phase A of the series

capacitor, the FFT block was adjusted from the base frequency adopted at 10 Hertz to the synchronous frequency, that is, (10, 20, 30, 40, 50 and 60Hz), as shown in Figure 13. It was possible to verify the predominance of the 40 Hertz frequency during and after the fault extinction, promoting the scenario of torsional oscillations. This scenario was repeated for the other phases of the capacitor.

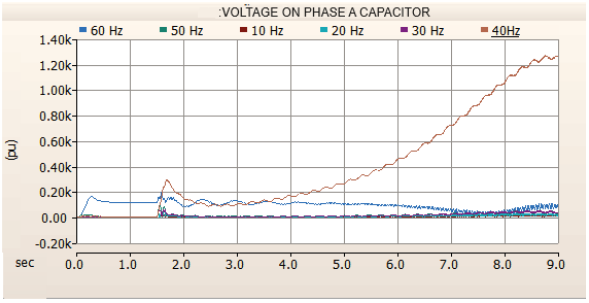

Figure 13. FFT analysis of the series capacitor voltage in phase A.

To obtain the frequency of the torque signals from the turbine-generator set for the 6 mass zones, the torque peak periods (in seconds) of the five adjacencies of the turbogenerator shaft were analyzed. According to the inverse relationship between period and frequency (f=1/T), the frequency of 20 Hertz can be verified through Figure 14, which represents a period of the waveform illustrated in Figure 9. Expanding the analysis to the other Torsional Interactions along the turbogenerator axis, there was a predominance of the frequency of 20 Hertz, with the occurrence of Torsional Interactions.

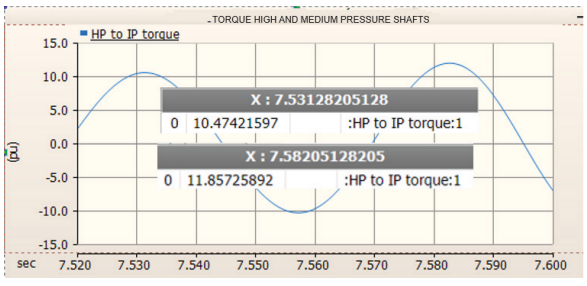

Figure 14. Periods of subsequent peaks – High and Medium Pressure Zones.

FOUL APPLIED AT POINT A

Applying the fault before the series capacitor, a scenario similar to the case of the fault applied at point B is observed. The disturbances and accentuation of the magnitudes of the electrical torque of the synchronous machine, the speed of the turbogenerator and overvoltage and overcurrent in the series capacitor were perpetuated. Of the latter, the worsening of disturbances in the stationary capacitive voltage signal stands out, culminating in magnitudes greater than 2000 pu, with an increase of 34% in relation to the previous fault point. Figure 15 illustrates this phenomenon.

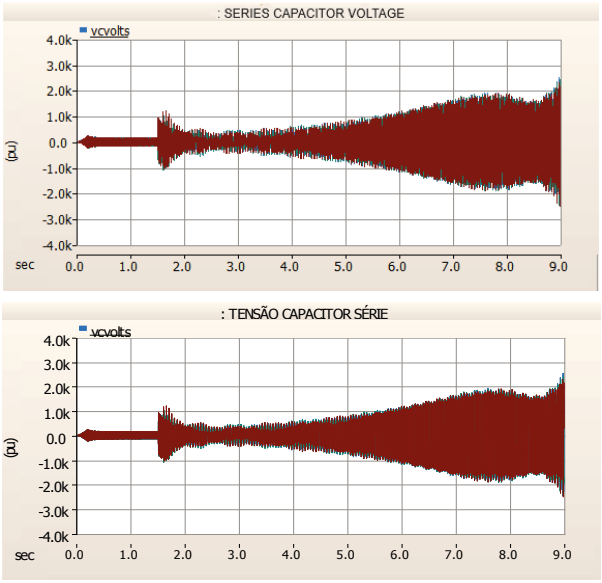

Figure 15. Voltage Signal in the Series Capacitor

Furthermore, in accordance with expectations, the torsional manifestations of the turbogenerator shaft showed behavior similar to the previous situation, with increased magnitudes. The torques between the LPB and generator sections and between IP and LPA are those that showed the highest percentage growth in relation to the fault in B, 74% and 34%, respectively. Figures 16 and 17 illustrate the described scenario. Regarding frequency values, no changes were observed,

with 40 Hz being the frequency value of the series capacitor quantities and 20 Hz being the frequency value of torsional manifestations.

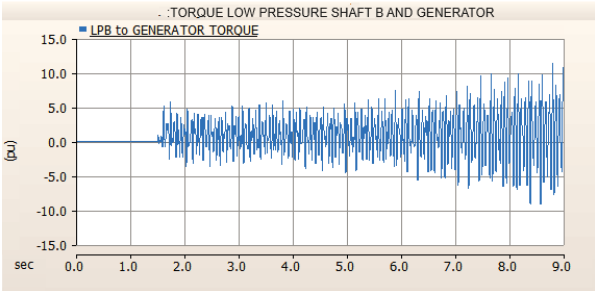

Figure 16. Torque between Low Pressure Zone B and Generator.

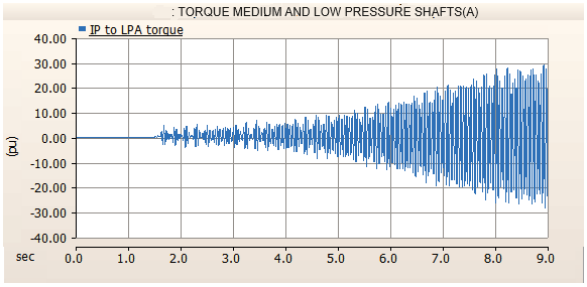

Figure 17. Torque between the Medium and Low Pressure Zones A.

COMPARATIVE ANALYSIS

According to the content exposed by the simulations, the phenomenon of Subsynchronous Resonance via Torsional Interactions was verified for the two fault points (A and B). The mechanical natural frequency of the turbogenerator of 20.21 Hz was sufficiently close to the frequency value of the shaft torques (20 Hz). To achieve this, the frequency value of the capacitor quantities was equal to the natural frequency of the electrical network of 40 Hz, resulting in a combined system frequency (synchronous frequency of 60 Hz minus the 40 Hz of the capacitor). This complementary frequency was responsible for inducing subsynchronous torques on the shaft at a frequency of 20 Hz. As the voltage stored for the fault before the series capacitor was higher, greater torsional interactions were witnessed. For the fault at point A, the largest torsional interactions occur, in descending order: between the low pressure zones, between generator-exciter, medium and low pressure A, high and medium pressure, low pressure zone B and generator. For the fault in B, the order was equivalent. The comparison between the magnitudes and parameters of the electromechanical system by fault location is illustrated in Table IV, considering the magnitude of the torques and the capacitor magnitudes in pu and the turbogenerator speed in *rad /sec.*

POI-NT	HP-IP	IP-LPA	LPA-LPB	LPB-GER	GER-EX	ω_c	V_c	I_c
A	14.7	29.5	48.8	11.4	41.0	456.6	2573	11
B	11	21	37	6.57	32.8	441	1920	8
A/B [%]	27	36	29	74	25	4	34	38

TABELA IV. COMPARISON BETWEEN MISSING POINTS

CONCLUSION

Subsynchronous Resonance is assessed by locating different points for imposing faults in the system. It must be noted that the applications of faults at the two different points indicated were considered specifying the same degree of compensation previously adopted. The modal analysis indicated the natural frequencies of oscillations relative to the system that were indicated in Table III, and these values were confirmed in the simulation results of the equivalent model in the PSCAD/EMTDC program [12]. When the fault is located before series compensation, the capacitor stores even more voltage, resulting in an accentuated discharge of subsynchronous currents in the turbogenerator, compared to the fault after the capacitor. This scenario, in addition to culminating in Torsional Interactions, proportional to the voltage stored by the capacitor, stimulates the induction of transient torques, resulting in Torque Amplification.

REFERENCES

[1] Ordóñez, Camilo Andrés, Antonio Gómez- Expósito, and José María Maza-Ortega. 2021. "Series Compensation of Transmission Systems: A Literature Survey" Energies 14, no. 6: 1717. https://doi.org/10.3390/en14061717

[2] RG FARMER et al, "Terms, Definitions and Symbols for Subsynchronous Oscillations IEEE Subsynchronous Resonance Working Group of the System Dynamic Performance Subcommittee Power System Engineering Committee," in IEEE Power Engineering Review, vol. PER-5, no. 6, pp. 37-37, June 1985, doi : 10.1109/MPER.1985.5526631.

[3] ANDERSON, PM; AGRAWAL, BL; VAN NESS, J.E.; " Subsynchronous Resonance in Power Systems", 2nd ed., New York, IEEE, 1996.

[4] OLIVEIRA, SEBASTIÃO E; DOS SANTOS, MG; " Subsynchronous Resonance : A form of electromechanical instability", II SEPOPE – Seminar for Specialists in Operation and Planning of Electrical Systems. Brazil – 1989.

[5] DOBSON, IAN; "Strong Resonance Effects in Normal Form Analysis and Subsynchronous Resonance", Bulk Power Dynamics and Control V, Onomichi, Japan, Aug, 2001.

[6] AA Fouad and KT Khu, " Subsychronous Resonance Zones in the IEEE "Bench Mark" Power System," in IEEE Transactions on Power Apparatus and Systems, vol. PAS-97, no. 3, pp. 754-762, May 1978, doi : 10.1109/TPAS.1978.354546.

[7] R. Rajaraman and I. Dobson, "Justification of torque per unit velocity methods of analyzing subsynchronous resonance and a swing mode in power systems," in IEEE Transactions on Circuits and Systems I: Fundamental Theory and Applications, vol. 45, no. 10, pp. 1109-1113, Oct. 1998, doi: 10.1109/ 81.728867.

[8] PM Anderson, RG Farmer, Series Compensation of Power Systems, California: PBLSH! Inc., 1996.

[9] R. G. Farmer, A. L. Schwalb and E. Katz, "Navajo project report on subsynchronous resonance analysis and solutions," in IEEE Transactions on Power Apparatus and Systems, vol. 96, no. 4, pp. 1226-1232, July 1977, doi : 10.1109/T-PAS.1977.32445.

[10] "First benchmark model for computer simulation of subsynchronous resonance," in IEEE Transactions on Power Apparatus and Systems, vol. 96, no. 5, pp. 1565-1572, Sept. 1977, doi : 10.1109/T-PAS.1977.32485.

[11] R. G. Farmer, "Second Benchmark Model for Computer Simulation of Subsynchronous Resonance IEEE Subsynchronous Resonance Working Group of the Dynamic System Performance Subcommittee Power System Engineering Committee," in IEEE Power Engineering Review, vol. PER-5, no. 5, pp. 34-34, May 1985, doi : 10.1109/MPER.1985.5526570.

[12] Manitoba HVDC Research Center Inc, *PSCAD User's Guide.* Manitoba, Canada : Manitoba HVDC Research Center Inc, 2010. Available: https://www.pscad.com/

[13] TAVARES, Carlos André Andrade Subsynchronous Resonance and Other Forms of Electromechanical Instability; 2005; Dissertation (Master's in Electrical Engineering) – Universidade Federal do Rio de Janeiro.

[14] KUNDUR, P; "Power System Stabilty and Control", 1st ed., New York, McGraw-Hill, 1994.

[15] K. Clark, "Overview of subsynchronous resonance related phenomena," PES T&D 2012, 2012, pp. 1-3, doi : 10.1109/ TDC.2012.6281503.

[16] "IEEE Guide for the Functional Specification of Fixed-Series Capacitor Banks for Transmission System Applications," in IEEE Std 1726-2013, vol., no., pp.1-120, 7 March 2014, doi: 10.1109/ IEEESTD.2014.6759723.

[17] The MathWorks, Inc. (2022). *MATLAB version: 9.13.0 (R2022b).* Accessed: January 01, 2023. Available: .

[18] SADEGHI, Roozbeh; KNIGHT, Andrew M. Emulating Subsynchronous Resonance using Hardware and Software Implementation. In: 2018 IEEE Electrical Power and Energy Conference (EPEC). IEEE, 2018. p. 1-6.